

Literature research

About bicycle tyre measurements and tyre models

by

Niels Baltus

in partial fulfillment of the requirements for the degree of

Master of Science
in Mechanical Engineering

at the Delft University of Technology.

Supervisor: Dr. ir. Arend L. Schwab

Abstract

A lot of research has been done on the behaviour of pneumatic tyres and this has led to various tyre models and a lot of measurement data. However, in the specific field of bicycle tyres, not so much measurement data is available. Andrew Dressel changed this, because he did many measurements under different conditions and with different tyres [1]. This data can be useful for modelling purposes, e.g., vehicle dynamic simulators or vehicle control systems.

Using the data for modelling means that a tyre model is needed. A large variety of models is available. The best known tyre model is Prof. Pacejka's Magic Formula, which is an empirical model. This model can accurately replicate the real behaviour, but in order to do that extensive testing has to be done to find the many coefficients. Another known tyre model is FTire, which is a finite element model. This model can also accurately replicate real tyre behaviour, but a lot of computing power is needed.

In this literature study several tyre models are investigated. Every model is classified as either an empirical model or a finite element model or somewhere in between. Also the complexity of the models will be considered and the possible applicability for bicycle tyres. Moreover, all the available literature about bicycle tyre measurements will be summarised in such a way that they can be compared to each other. Interesting literature outside the scope of models and measurements, will also be summarised, because this might be useful for the Master thesis.

The models that classify as simple physical models, will be elaborated further in the Master thesis report. The goal is to use one of these models and find the model parameters corresponding to the measurements done by Dressel and the bachelor group. With the obtained model parameters it is expected that estimations for the behaviour of other bicycle tyres can be made.

Contents

Abstract	iii
1 Introduction	1
1.1 Bicycle tyres	1
1.1.1 Behavioural expectancy of a bicycle tyre	1
1.1.2 Bicycle tyre measurements	1
1.2 Research objectives and contributions	2
1.3 Fields of interests	2
1.3.1 Bicycle tyre measurements	2
1.3.2 Tyre models	2
1.3.3 Additional literature	2
1.4 Literature survey outline	2
2 Bicycle tyre measurements	3
2.1 1972 - R. Douglas Roland	3
2.2 1975 - J.A. Davis	3
2.3 1979 - G. K. Man and T. R. Kane	3
2.4 1987 and 1988 - C.R. Kyle	4
2.5 2001 - D.J. Cole and Y.H. Khoo	5
2.6 2006 - V. Cossalter	5
2.7 2008 - R.S. Sharp	6
2.8 2012 - A. Doria	6
2.9 2013 - A. E. Dressel	7
2.10 2014 - J. Knuit, F. de Kok, P. Raaphorst, and A. van der Spek	7
3 Tyre models	9
3.1 1949 - Rotta model	10
3.1.1 Force generation	11
3.1.2 Model type	11
3.2 1952 - Tyre brush model	12
3.2.1 Force generation	14
3.2.2 Model type	16
3.3 1989 - Magic Formula tyre model	16
3.3.1 Force generation	17
3.3.2 Model type	18
3.4 1999 - Ftire	18
3.4.1 Force generation	18
3.4.2 Model type	20
3.5 2005 - Enhanced string model	20
3.5.1 Force generation	20
3.5.2 Model type	21
3.6 2001 - RMOD-K	21
3.6.1 Force generation	21
3.6.2 Model type	21
3.7 2016 - Nonlinear brush formulation for a bicycle tire based on the Rotta model	21
3.7.1 Force generation	22
3.7.2 Model type	22
3.8 2017 - Non-smooth delayed contact model	22
3.8.1 Force generation	24
3.8.2 Model type	24

4	Additional literature	25
4.1	Motorcycle research	25
4.1.1	1971 - R.S. Sharp	25
4.1.2	1976 - R.S. Rice and D.T. Kunkel	25
4.1.3	1979 - H. Sakai, O. Kanaya and H. Iijima	25
4.1.4	1998 - E.J.H. De Vries and H.B. Pacejka	26
4.1.5	2002 - R. Berrirra, V. Cossalter A. Doria and Lot	26
4.2	Books	26
4.2.1	1981 - Mechanics of pneumatic tires	26
4.2.2	2006 - The pneumatic tire	26
4.3	Miscellaneous	26
4.3.1	1991 - Pacejka and Sharp	26
5	Conclusions	27
	Bibliography	29

1

Introduction

A tyre transfers the vehicle's load from the axle through the wheel to the surface over which it travels and provides traction. Most tyres, such as car, aircraft and bicycle tyres are pneumatically inflated rubber structures. It is this composition that makes tyres do what they are meant to do; provide traction in longitudinal and lateral direction and absorb shocks in vertical direction. However, it is also this composition that makes the behaviour of tyres highly non-linear. This non-linear behaviour makes it hard to model a tyre. A lot of research has been done on the behaviour of pneumatic tyres and this has led to various tyre models. These tyre models can be divided into two groups: phenomenological models and physical models [2]. The phenomenological models are based on experimental data and the physical models are theory based. Naturally, combinations of both models also exist.

Nowadays, the phenomenological model developed by Prof. Dr. Ir. Pacejka, the Magic Formula, for forces generated in tyre contact patches is widely used, since this model can approximate the tyre forces quite accurately. The disadvantage is that they are not based on physical properties of the tyre and a lot of measurements are needed to find the values of the large amount of parameters that describe the tyre behaviour.

A physical model, FTire [3], is a finite element method computer simulation. This model also approximates the tyre forces accurately. Here the disadvantage is that it cannot run accurate simulations in real-time. A lot of processing power is needed to calculate the tyre forces.

1.1. Bicycle tyres

1.1.1. Behavioural expectancy of a bicycle tyre

Bicycle tyres are expected to behave more simply than car or truck tyres. Car and truck tyres have steel belts and a thick carcass, which causes more non-linear effects in their behaviour and makes the modelling more complex. A bicycle tyre is slender when the contact patch width is compared to the wheel radius and the contact patch length. A bicycle tyre is also circular in cross section, which suggests a simpler geometry [4]. Most bicycle tyres for urban purposes also have a thin casing with almost no bending stiffness (non-inflated). This behavioural expectancy suggests easier tyre modelling, where less model parameters are needed to describe the tyre behaviour.

1.1.2. Bicycle tyre measurements

In 2013 Andrew Dressel received the Degree of Doctor of Philosophy in Engineering at the University of Wisconsin-Milwaukee by presenting his research: Measuring and modeling the mechanical properties of bicycle tires [1]. In this research he did a lot of measurements with multiple bicycle tyre brands and models. The results from these measurements are interesting to use for modelling purposes. In addition to this research a group of bachelor students examined the vertical stiffness under different conditions [5] of the same bicycle tyres as used by Dressel. This increases the usefulness for modelling purposes, because a more complete data set is available.

1.2. Research objectives and contributions

This research aims to contribute to the understanding of bicycle tyre behaviour, in particular the effect that tyre properties have on this behaviour. In this case tyre properties refer to properties like inflation pressure, tyre width, vertical load and rubber compound. Tyre behaviour refers to behavioural properties like cornering stiffness, camber stiffness and vertical stiffness. The many bicycle tyre measurements done by Dressel and the available tyre models hopefully can be combined such that this research contributes to the understanding of bicycle tyre behaviour.

1.3. Fields of interests

In order to contribute to the field of bicycle tyre dynamics and not repeat existing researches, it is good to know what literature is available. Moreover, this literature might contain essential information which can be used later on in this research. There are two fields in particular that are interesting to look into.

1.3.1. Bicycle tyre measurements

Besides Andrew Dressel there are others that have performed experiments in order to find the influence of tyre properties on its behaviour. An overview of the published literature will be made in this research. Results of those researches also might be useful for this research, just like the results from Dressel.

1.3.2. Tyre models

In this literature survey there will also be an overview of what has been done in the field of tyre modelling. These models will most likely already give a good indication of how the tyre properties influence the behavioural properties. There also might be a possibility to use one or more of the models in combination with the results of conducted experiments from other researches.

1.3.3. Additional literature

During the literature survey, it is possible to stumble upon interesting researches which are not particularly in one of the categories above. Evidently, these researches will also be discussed.

1.4. Literature survey outline

This literature survey will outline the proposed fields of interests and explore current and previous developments using available literature. In Chapter 2 an overview is given of researches that conducted experiments concerning bicycle tyre behaviour. In Chapter 3 various tyre models will be discussed. Chapter 4 will describe the additional literature that has been found and how it can benefit this research.

2

Bicycle tyre measurements

In this Chapter previously executed bicycle tyre measurements will be discussed. The researches will be ordered chronologically. Many of these researches have been mentioned by Dressel already.

2.1. 1972 - R. Douglas Roland

Roland is the first to report the results of measured bicycle tyres [6]. The measured were carried out at the Calspan Corporation with a single-wheeled trailer towed behind a car on an asphalt road surface. The normal load was supplied by fixing weights to the trailer. Extensive corrections were required in the resultant data, since normal load, slip angle and camber angle were not independent variables. They all influence each other to a certain amount and they were also affected by the level of side force. Eleven different tyres ranging from 24 to 27 inches wheel diameter have been tested. He used pressures from 3.8 to 7.6 bar and normal loads from 15.9 to 68 kg. The normalised cornering stiffness that was found was between 0.15 and 0.35 per degree of slip angle and the normalised camber stiffness was between 0 and 0.1 per degree of camber angle.

2.2. 1975 - J.A. Davis

Davis continues the bicycle tyres testing at Calspan [7]. However, to improve the repeatability and accuracy of the measurements he uses a 1.22 meter diameter drum. The focus of this research shifts more towards measurements on wet pavement and with low inflation pressures. Davis uses 4 different tyres from which one is the same as Roland used. He did a duplicate test with this tyre with normal loads of 22.68 and 45.36 kg. The test Roland did was with 34.02 kg, so this is exactly in between the loads that Davis used. For this particular tyre (Puff Road Racer at 5.17 bar) Roland found a normalised cornering stiffness of 0.167. Davis found values of 0.200 and 0.160 for normal loads of 22.68 and 45.36 kg respectively. So this corresponds fairly well with each other.

The camber stiffness found by Davis is harder to report, because the graphs for the camber stiffness are non-linear. For example, for the Puff Road Racer at 5.17 bar and 45.36 kg, the lateral force at 10 degree inclination angle is 0.90 kg, which comes down to a camber stiffness of 0.002 per degree of camber. For the same tyre and conditions the lateral force at 20 degree inclination angle the lateral force is 2.27 kg, which comes down to a camber stiffness of 0.0075 per degree of camber.

Observations on the dry tyre tests reported by Davis are:

- Decreasing inflation pressure shows a noticeable decrease in cornering stiffness. This effect is not observed for camber stiffness.
- Normalised side force decreases with increasing normal force, which agrees to previous tyre test results.

2.3. 1979 - G. K. Man and T. R. Kane

This research was conducted at the Mechanical Engineering Department of Stanford University [8]. The normalised values found by Man and Kane are 0.22 per degree of slip angle and 0.00325 per

degree of camber angle.

2.4. 1987 and 1988 - C.R. Kyle

The research done by Chester R. Kyle, Ph.D., Adjunct Professor of Mechanical Engineering at the California State University, from which it is not sure if it was ever published, contains a variety of tested tyres. The PDF documents in which the results are presented are obtained from Dr. ir. Arend L. Schwab, my supervising professor. The research is conducted at the facilities of General Motors and is mostly focused on rolling resistance. The first document from 1987 [9], presents data for a "small" tyre with an outside diameter of 0.44 m on a 1.7 m drum at 3.5 kph. The stiffness values reported are summarised in Tables 2.1, 2.2 & 2.3.

Table 2.1: Normalised cornering stiffness values at 1 degree slip for a small tyre reported by Kyle in 1987.

	Load [N]		
Pressure [bar]	300	450	600
5.17	0.213	0.179	0.157
6.89	0.244	0.216	0.183
7.79	0.201	0.173	0.156

Table 2.2: Normalised self-aligning torque stiffness values at 1 degree slip (mm) for a small tyre reported by Kyle in 1987.

	Load [N]		
Pressure [bar]	300	450	600
5.17	2.37	2.78	2.83
6.89	2.23	2.4	2.53
7.79	2	2.2	2.33

Table 2.3: Normalised camber stiffness values at 1 degree camber for a small tyre reported by Kyle in 1987.

	Load [N]		
Pressure [bar]	300	450	600
6.89	0.0166	0.0156	0.0142

The other document from 1988 reports mainly about tyre rolling resistance, but it includes also some stiffness values for a 17 inch x 1¹/₄ inch Moulton tyre [10]. These values are shown in Table 2.4.

Table 2.4: Normalised cornering stiffness values at 1 degree slip for a Moulton 17x1¹/₄ reported by Kyle in 1988.

	Load [N]		
Pressure [bar]	300	450	600
7.79	0.202	0.175	0.161

Some observations reported by Kyle are:

- The cornering force on a rough stable surface will increase with higher tyre loads.
- Higher pressure can have varying results. Cornering force can reach a maximum and decline with increasing pressure.
- Slick treads have a higher cornering force than patterned treads on dry roads.
- The effect of tyre width on cornering force is unclear.

2.5. 2001 - D.J. Cole and Y.H. Khoo

Cole and Khoo used a back-to-back tyre test device to measure cornering stiffness, a schematic drawing of this device is shown in Figure 2.1. They tested 57-406 20 inch diameter and 2.125 inch tyre width at 2.4 bar and under 132-623 N vertical load. The results are summarised in Table 2.5.

Table 2.5: Normalised cornering stiffness values for a 20 inch diameter and 2.125 inch width tyre reported by Cole and Khoo in 2001.

Slip angle [degrees]	Load [N]					
	132	231	329	427	525	623
1	-	0.22	0.21	0.17	0.16	0.13
2	-	-	0.35	0.31	0.28	0.24
3	-	-	-	0.4	0.35	0.32

The forward speed is not mentioned and the camber angle had been set to zero for all the tests. Note: They reported their results in a very unusual way. I am not sure if I interpreted the results good now, but for me it seems the most logical in this way. With unusual I mean that apart from the largest normal force, all others seem to have a negative lateral force at non-zero slip angles [11].

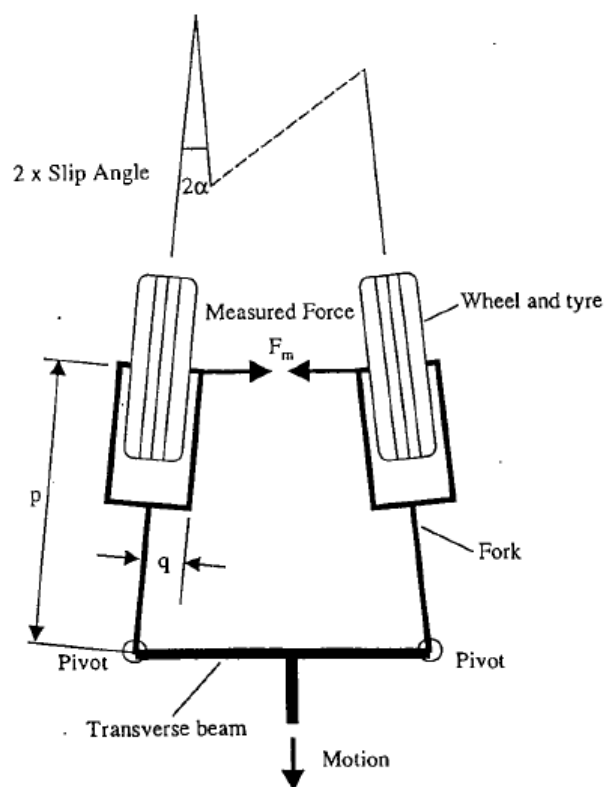


Figure 2.1: Schematic drawing of the back-to-back tyre measurement device ¹.

2.6. 2006 - V. Cossalter

In his book Motorcycle Dynamics [12], Cossalter shows the results from a racing bicycle tyre compared to scooter and motorcycle tyres. The brand, model, forward speed, normal load and inflation pressure are not reported. The measurements were executed on a rotating disk machine [13]. The values he found are shown in Tables 2.6 & 2.7.

¹Image is taken from [11].

Table 2.6: Normalised cornering stiffness values reported by Cossalter.

Side slip angle [degree]	1	2	3
Normalised lateral force	0.09	0.18	0.28

Table 2.7: Normalised cornering stiffness values reported by Cossalter.

Camber angle [degree]	5	10	15	20	25	30	35	40
Normalised lateral force	0.07	0.15	0.23	0.30	0.38	0.48	0.61	0.65

2.7. 2008 - R.S. Sharp

In the paper "On the Stability and Control of the Bicycle" [14], Sharp used tyre measurement results from Roland to estimate aligning moments. For the normalised cornering stiffness he uses 0.25 and he mentions that the camber stiffnesses measured by Roland were "unreasonably large", such that he will use the tangent rule for side force generated by the camber angle.

2.8. 2012 - A. Doria

Doria tested four tyres [15] on the rotating disk machine at the University of Padua [13]. Vertical loads of 400 N & 600 N were used and the forward velocity was 4 km/h. The tested tyres are shown in Table 2.8.

Table 2.8: Measured tyres by Doria.

Tyre	Size	Type	Recommended inflation pressure [bar]	Bead
1	37-622	Diagonal	4.0-6.0	Wire
2	37-622	Diagonal	3.8-5.5	Wire
2	35-622	Diagonal	4.0-6.5	Wire
4	37-622	Diagonal	4.0-6.0	Folding

The results of the side-slip force measurements are shown in Table 2.9 and the results of the camber force measurements are shown in Table 2.10. It seems that these measurements were performed with 400 N normal load and 4 bar inflation pressure, they did not mention it, but looking at the results of inflation pressure and normal load influence where they did mention the conditions, the measurement conditions seem to be like this.

Table 2.9: Normalised side-slip force as measured by Doria.

Slip angle [degree]	0.5	1	1.5	2	2.5	3	3.5	4
Tyre 1	0.04	0.24	0.36	0.46	0.56	0.64	0.71	0.77
Tyre 2	0.04	0.22	0.34	0.44	0.53	0.61	0.68	0.74
Tyre 3	0.05	0.20	0.33	0.44	0.55	0.64	0.73	0.81
Tyre 4	0.03	0.16	0.23	0.30	0.37	0.44	0.49	0.54

Table 2.10: Normalised camber force as measured by Doria.

Camber angle [degree]	2	4	6	8	10	12	14	16	18	20	22	24
Tyre 1	0.03	0.10	0.14	0.19	0.25	0.31	0.36	0.40	0.47	0.52	0.52	0.49
Tyre 2	0.02	0.10	0.16	0.18	0.24	0.30	0.35	0.39	0.45	0.50	0.52	0.54
Tyre 3	0.05	0.10	0.13	0.18	0.22	0.28	0.32	0.37	0.45	0.50	0.56	0.59
Tyre 4	0.02	0.06	0.09	0.12	0.16	0.20	0.23	0.26	0.30	0.33	0.36	0.40

2.9. 2013 - A. E. Dressel

The motivation for this research came from the work that Dressel published in 2013 [1]. In this research he measured a lot of bicycle tyres and reported all of the conditions and variables, which makes it very useful for modelling purposes. A list of measured tyres is shown in Table 2.11.

The measured normalised cornering stiffness varies from below 0.15 to over 0.35 per degree of slip angle. This is $\pm 40\%$ from the average. The normalised camber stiffness varies from below 0.0075 to 0.015 per degree of camber angle. This is $\pm 33\%$ from the average.

Dressel also further develops a numerical model based on the Rotta model to get more insight in how slender toroidal tyres in contact with the ground generate the forces and attempts to predict them from simpler measurements. Even though the actual values generated by the model do not exactly match the measured values, the trends in lateral stiffness values and contact patch size do correspond with the measured data as parameters like the inflation pressure, vertical load and rim width vary.

Table 2.11: The tyres that Andrew Dressel tested.

Brand	Model	Size	Tread	Bead
Bontrager	All Weather	23	Semi-smooth	Foldable
Bontrager	All Weather	25	Semi-smooth	Foldable
Bontrager	All Weather	28	Semi-smooth	Foldable
Cheng Shin	Classic Zeppelin	50	-	Wire
Continental	Top Contact Winter	37	-	Wire
Maxxis	Radial Prototype	22	Smooth	Foldable
Michelin	Dynamic	23	Semi-smooth	Wire
Schwalbe	Big Apple	55	-	Wire
Schwalbe	Kojak	35	-	Foldable
Schwalbe	Marathon Plus	37	-	Wire
Vittoria	Randonneur Hyper	37	-	Foldable
Vredestein	Perfect Tour	37	Semi-smooth	Wire
Vredestein	Fortezza DuoComp	23	Smooth	Foldable
Vredestein	Fortezza TriComp	23	Smooth	Foldable

2.10. 2014 - J. Knuit, F. de Kok, P. Raaphorst, and A. van der Spek

As comprehensive the research by Dressel [1] is, he forgot to measure the vertical stiffness of each tyre. Therefore, a Bachelor end project had the goal to measure the vertical stiffness of the same tyres measured by Dressel, using the same vertical loads and inflation pressures. Just like Dressel, this group also reported all the conditions and variables very well [5]. Due to this additional research the data is even more useful for modelling purposes.

3

Tyre models

In this Chapter various tyre models will be discussed. The tyre models will be ordered chronologically. As was mentioned in Chapter 1, there are two main groups of tyre models: phenomenological models and physical models. Figure 3.1 from "Tire and Vehicle Dynamics" [2] gives a good overview of several properties of the model groups. The models discussed in this Chapter will be placed in this graph to understand its properties.

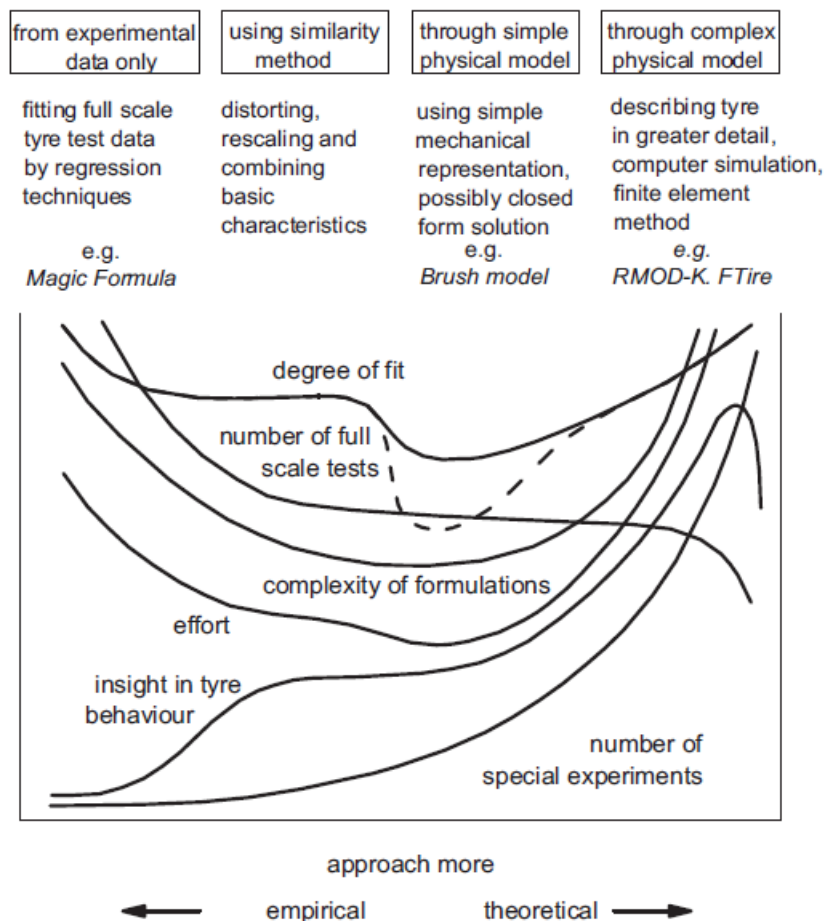


Figure 3.1: Four categories of possible types of approach to develop a tyre model¹.

¹Image taken from [2].

3.1. 1949 - Rotta model

Rotta developed a sectional model of an infinitesimal slice of rim and tyre [16]. The model consists of two parts: the rim and the tyre. The rim is represented by a rigid line segment and the tyre is represented by an inextensible string. They are connected at the rim edges. Inside there is a pressure p . When the tyre is not in contact with the ground, the cross-section of the tyre and rim looks like Figure 3.2, with B as the tyre width and H the tyre height.

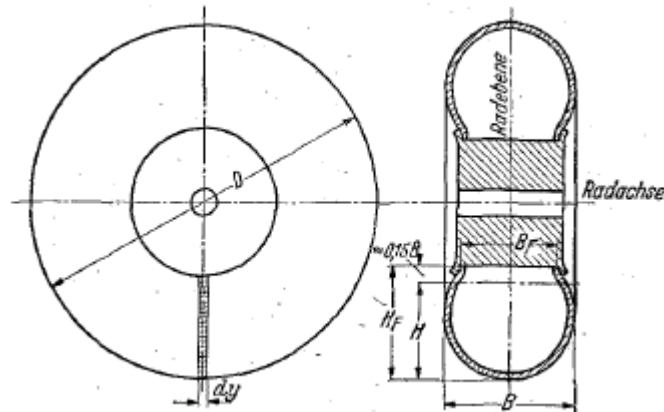


Figure 3.2: Tyre dimensions and definitions as used by Rotta².

When the tyre is placed on the ground and a load is put on the rim, the symmetrical deformation becomes like shown in Figure 3.3. In this figure B_r is the rim width, γ the angle at which the string leaves the rim, r the radius of the deformed tyre, f the vertical deflection of the tyre and b the contact width of the tyre.

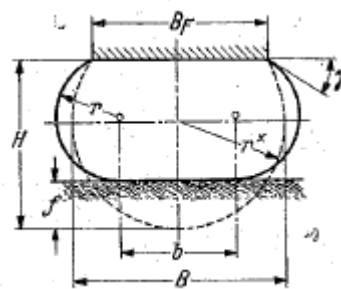


Figure 3.3: Symmetrical tyre flattening³.

Then there is the situation where the tyre is in contact with the ground and a side-slip angle is induced such that the cross-section of the tyre is not symmetrical anymore. This situation is shown in Figure 3.4, where each side of the tyre arc has a different radius and angle at which it leaves the rim.

²Image taken from [16].

³Image taken from [16].

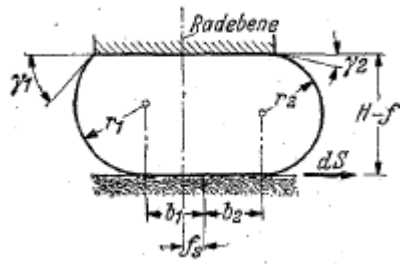


Figure 3.4: Non-symmetrical tyre flattening due to induced slip angle⁴.

Lastly, there is the situation where the tyre is in contact with the ground and a camber angle is induced. This is depicted in Figure 3.5, where there is again a difference in side wall radius and angle at which the tyre string leaves the rim.

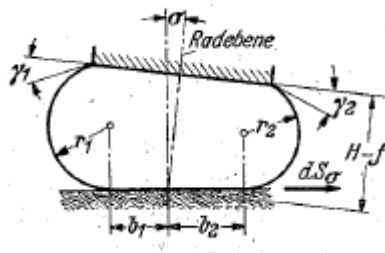


Figure 3.5: Non-symmetrical tyre flattening due to induced camber angle⁵.

Now if it is assumed that the length of the tyre string does not change, the sum of both side wall arcs and the ground contact patch is a fixed number, in any state of the tyre. Using geometry it is possible to find the relation between the known parameters (rim width, vertical deflection, tyre string length, horizontal difference between rim midpoint and ground contact midpoint and camber angle of the rim) and the unknown parameters (side wall radii, ground contact length and angle at which the tyre leave the rim). The extensive equations can be found in [16] or in [17] for the English version.

3.1.1.1. Force generation

Once the unknown parameters are calculated the vertical force for the cross-section is equal to the ground contact width times the pressure.

$$dF_z = p(b_1 + b_2)dy \tag{3.1}$$

The horizontal force is derived from the two different sidewall tensions. The sidewall tension is computed as $T = pr$. So the horizontal force is equal to the difference in sidewall arc length times the pressure.

$$dF_x = p(r_1 - r_2)dy \tag{3.2}$$

For getting the total vertical and horizontal force on the tyre all that has to be done is to sum up the separate cross-sections.

$$F_z = \sum dF_z \text{ and } F_x = \sum dF_x \tag{3.3}$$

3.1.1.2. Model type

The Rotta model is a geometric model which would classify as a simple physical model in the graph from Figure 3.1. This model is only valid for tyres that have a circular cross-section, e.g. bicycles, aeroplanes and to some extent motorcycle tyres.

⁴Image taken from [16].

⁵Image taken from [16].

3.2. 1952 - Tyre brush model

The tyre brush model is a relatively simple theoretical tyre model. The original “brush” model was developed by Fromm and Julien (1952). This model did not consider carcass compliance. Fiala (1954) and Freudenstein (1961) developed theories in which the carcass deflection is approximated by a symmetric parabola. Böhm (1963) and Borgmann (1963) used asymmetric approximate shapes determined by both the lateral force and the aligning torque. Pacejka (1966, 1981) established the steady-state side-slip characteristics for a stretched-string-tyre model. The different theories of the various one-dimensional models have been compared by Frank (1965). In his research he compares: 1. stretched-string model, 2. beam model, 3. Fiala’s model (symmetric parabolic carcass deflection and 4. the model of Fromm (brush model with rigid carcass). The results are shown in Figure 3.6. The tread element stiffness is the same for each model and the parameters of each model have been chosen in such a way that they give the best fit to the experimental data for the peak side force and the cornering force for small slip angles. From this research can be concluded that when the parameters are chosen properly, the choice of tyre model has only a limited effect.

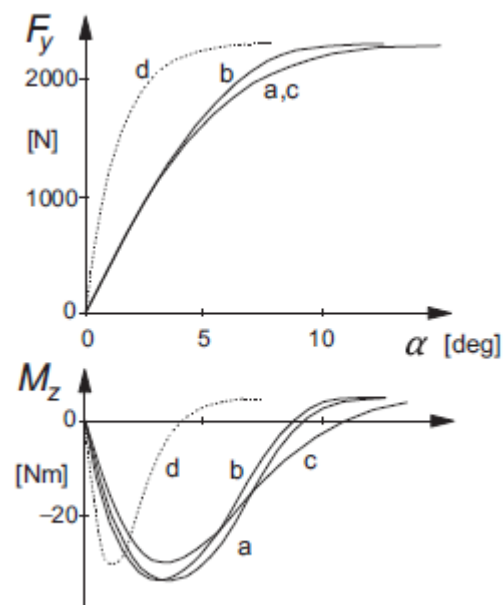


Figure 3.6: Comparison of calculated characteristics for four different tyre models with tread elements and non-symmetrical pressure distribution at a given wheel vertical load (a: string, b: beam, c: Fiala, d: brush with rigid carcass)⁶.

In the brush model the tyre is represented by a row of elastic bristles that touches the road plane. The bristles can be seen as the tread elements and are able to deflect in a direction parallel to the road surface. The flexibility of the bristles represents the elasticity of the combination of carcass, belt and actual tread elements of the real tyre. The first element of a rolling tyre that enters the contact zone is assumed to stand perpendicular to the road surface. For a freely rolling tyre in upright position (no camber angle), so no turning (no side-slip angle), accelerating or braking (no tyre slip), all elements are perpendicular to the road surface and in this case they are not generating a force. Rolling resistance will be ignored for the sake of simplicity. In the case that the wheel velocity vector V has an angle with respect to the wheel plane, side-slip occurs. Fore-and-aft slip occurs when the rotational wheel velocity multiplied with the effective rolling radius is not equal to the forward component of the wheel velocity. The combined slip situation is shown in Figure 3.7. The deflection of the elements induce forces and depending on the position of the resultant force, a moment occurs as well. In Figure 3.8 pure side-slip situations are shown. As can be seen there is a maximum amount of possible deflection depending on the position in the contact region of the element. This is determined by the vertical force distribution. The maximum force that can be generated by the tyre depends on three parameters: the friction coefficient μ , the vertical force distribution q_z and the stiffness of the element c_{py} . The vertical

⁶Image taken from [2].

force distribution is assumed to be parabola shaped. With this the maximum deflection is also parabola shaped. As shown in Figure 3.8 there are two possible states for the contact region: adhesion and sliding. The point where the straight line intersects the parabola is the point from where the sliding starts. By increasing the slip angle, the generated side force increases. The position from the resultant force behind the contact centre is called the pneumatic trail t . The aligning torque is generated by the non-symmetric shape of the deflection distribution and can be calculated by multiplying the lateral force with the pneumatic trail. The characteristics of the lateral force and aligning torque at increasing side-slip angle are shown on the right side of Figure 3.8.

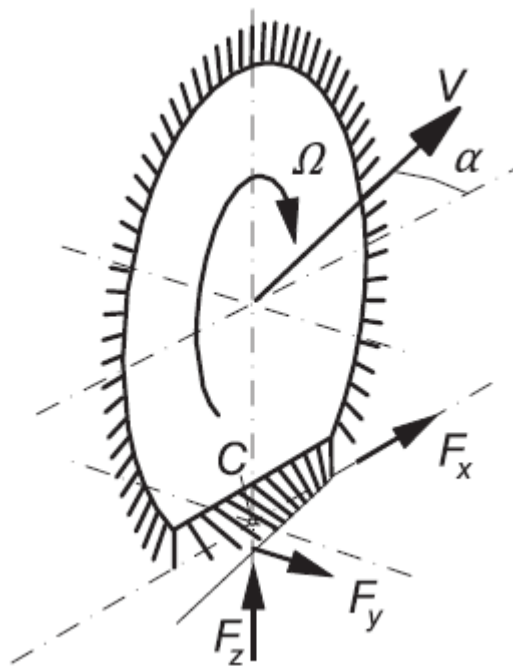


Figure 3.7: A visual representation of both slip situations in the brush tyre model ⁷.

⁷Image is taken from [2].

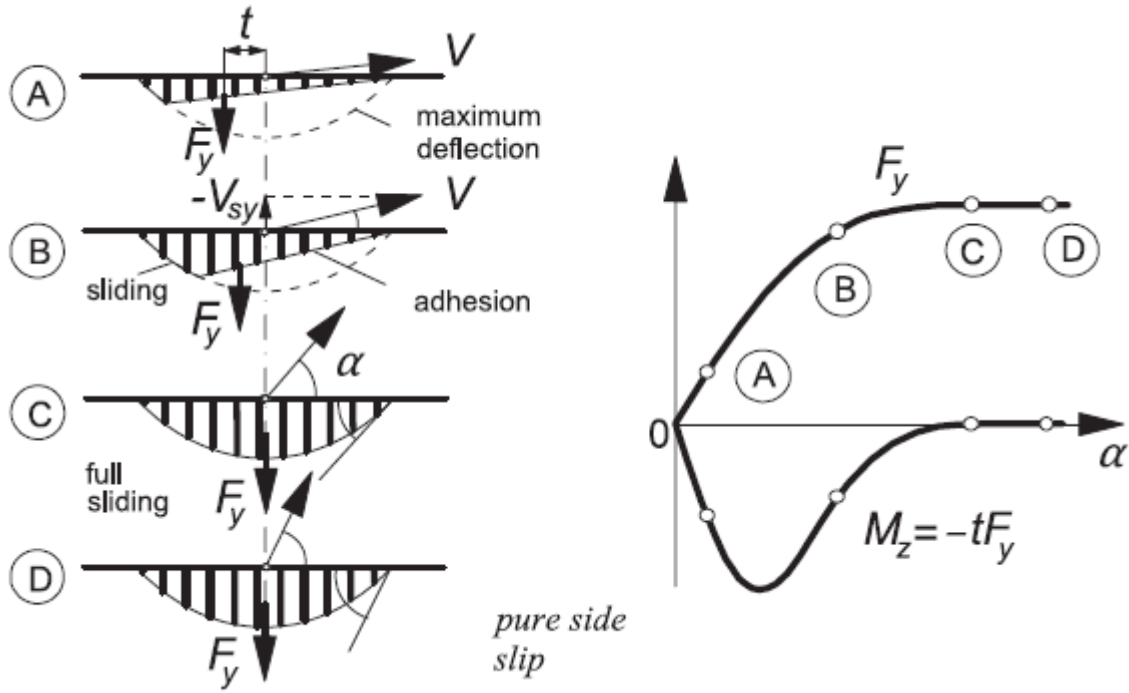


Figure 3.8: Left: Pure side-slip, from small to large slip angle. Right: Resulting side force and aligning torque characteristics ⁸.

3.2.1. Force generation

Pure side slip

A more detailed visualisation of the tyre brush model moving at a constant slip angle is depicted in Figure 3.9. The contact line in the adhesion range is straight and parallel to the velocity vector V and in the sliding range it is curved, since the available frictional force becomes lower than the force which would be required for the tips of the tread elements to follow the straight line further. The lateral deformation in the adhesion range equals

$$v = (a - x) \tan \alpha \quad (3.4)$$

where a is half the contact length. For $\alpha \rightarrow 0$ or $\mu \rightarrow \infty$, the sliding region vanishes and Equation 3.4 is valid for the entire contact region. The following integrals and expressions for the cornering force F_y and the self-aligning torque M_z hold:

$$F_y = c_{py} \int_{-a}^a v dx = 2c_{py}a^2\alpha \quad (3.5)$$

$$M_z = c_{py} \int_{-a}^a vx dx = -\frac{2}{3}c_{py}a^3\alpha \quad (3.6)$$

where c_{py} is the stiffness of the tread elements per unit length of the assumedly rectangular contact area.

⁸Image is taken from [2].

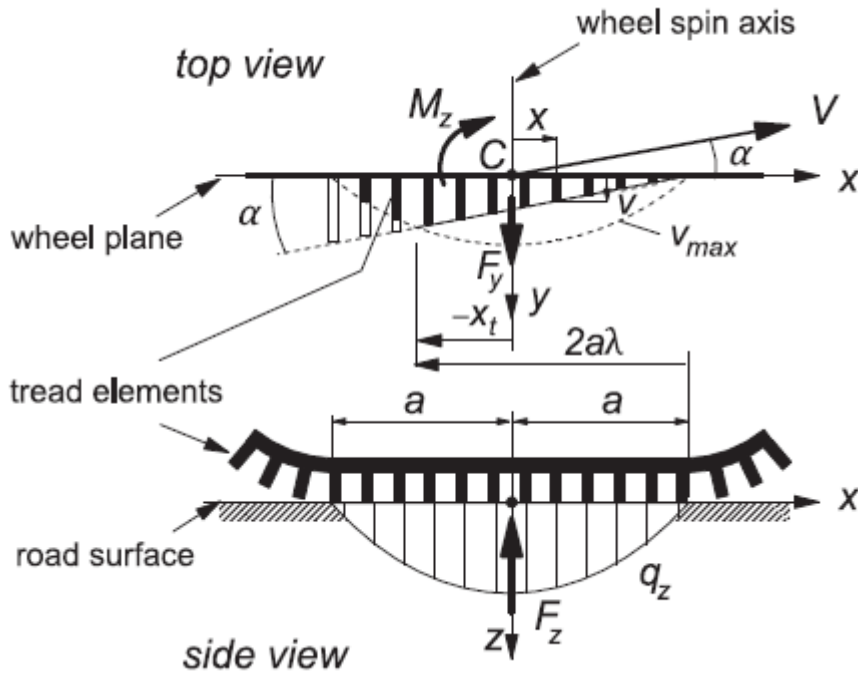


Figure 3.9: Top and side view of the tyre brush model moving at pure slip angle ⁹.

Camber and turning

Along with longitudinal slip (slip ratio) and lateral slip (slip angle) there is a third slip quantity which is called spin. The total spin consists of two components: camber and turn slip. This third slip quantity is described by Pacejka in [18]. In Figure 3.10 a visualisation of spin is depicted, with γ indicating the camber angle, the yaw angle ψ , path radius R and the wheel rotational velocity Ω .

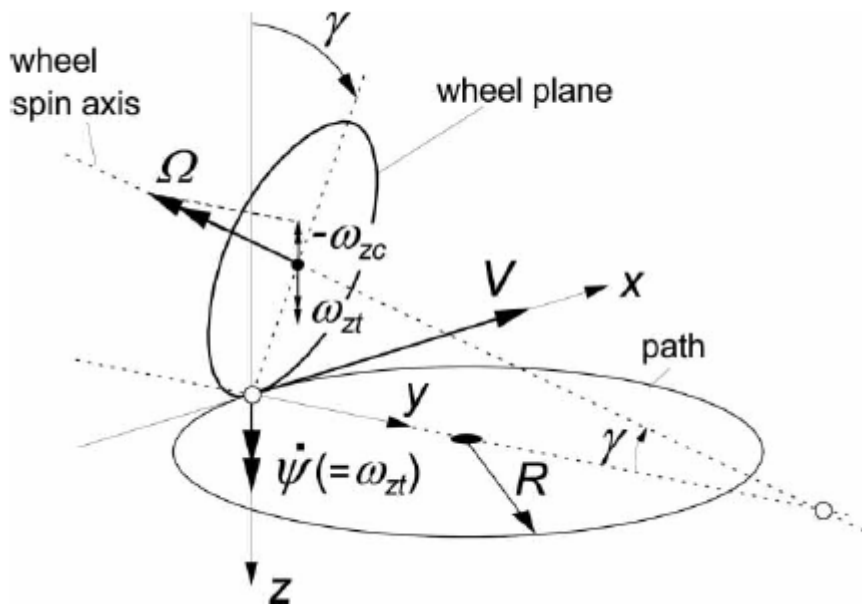


Figure 3.10: Pure turn slip and camber ¹⁰.

⁹Image is taken from [2].

The normal component of the rotational velocity ω_z over the forward velocity V is called the spin slip φ . For a freely rolling wheel (no braking, driving or side slip), the following equation is valid:

$$\varphi = -\frac{1}{V}\omega_z = -\frac{1}{V}(\dot{\psi} - \Omega \sin \gamma) = -\frac{1}{R} + \frac{1}{r_e} \sin \gamma \quad (3.7)$$

The total spin in fact is just the difference of two curvatures: one of the path of the contact centre and the other of the vertical projection of the peripheral line of the undeformed tilted tyre.

When wheel is travelling in a straight line with a forced camber angle. This means that the wheel is not rotating around its z-axis, such that $\dot{\psi}$ is equal to zero. The spin slip becomes:

$$\varphi = \frac{1}{V}\Omega \sin \gamma = \frac{1}{r_e} \sin \gamma \quad (3.8)$$

The lateral force and the self-aligning torque respectively are:

$$F_y = C_{F\alpha} \alpha + C_{F\varphi} \varphi \quad (3.9)$$

$$M_z = -C_{M\alpha} \alpha + C_{M\varphi} \varphi \quad (3.10)$$

So when there is no side slip, Equation 3.9 & 3.10 can be reduced to:

$$F_y = C_{F\varphi} \varphi \quad (3.11)$$

$$M_z = C_{M\varphi} \varphi \quad (3.12)$$

In the article by Pacejka [18] reciprocity is observed in the moment response to side-slip and the force response to turn slip. For the tyre brush model it turns out that

$$C_{F\varphi} = C_{M\alpha} \quad (3.13)$$

With this information the force generated by camber becomes:

$$F_y = C_{F\varphi} \frac{1}{r_e} \sin \gamma = C_{F\varphi} \frac{1}{r_e} \gamma = \frac{2}{3} \frac{1}{r_e} c_{py} a^3 \gamma \quad (3.14)$$

3.2.2. Model type

The tyre brush model is classified as a simple physical model in the graph from Figure 3.1. Depending on the type of tyre, the model with or without carcass compliance can be used.

3.3. 1989 - Magic Formula tyre model

In 1989 Bakker and Pacejka published a paper in which they developed a formula that could capture the steady-state tyre characteristics [19]. By testing and evaluating various improvements and extensions have been made over time [20–23]. The steady-state tyre characteristics are depicted in Figure 3.11. This formula is now widely used and is called "Magic Formula".

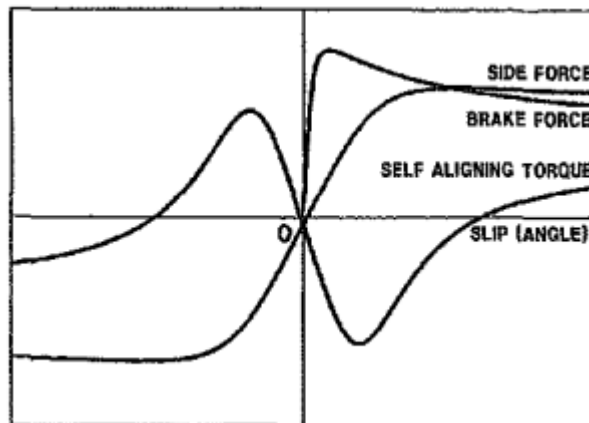


Figure 3.11: Steady-state tyre characteristics ¹¹.

¹⁰Image is taken from [18].

3.3.1. Force generation

The Magic Formula is given by the following equation:

$$\begin{aligned} y(x) &= D \sin(C \arctan(Bx - E(Bx - \arctan(Bx)))) \\ Y(X) &= y(x) + S_v \\ x &= X + S_h \end{aligned} \quad (3.15)$$

With $Y(X)$ standing for either side force, self-aligning torque or brake force and X denoting slip angle α or longitudinal slip κ .

The coefficients from equation 3.15 will be explained using the side force characteristic from Figure 3.12. D is the peak value and the product BCD equals the cornering stiffness at zero slip. Coefficient E makes it possible to accomplish a local extra stretch or compression of the curve in such a way that the stiffness and the peak value remain unaffected. Coefficient C defines the extent of the sine function which will be used and therefore determines the shape of the curve. The value of C makes the curve look like a side force, brake force or a self-aligning torque characteristic. Due to ply steer, conicity, rolling resistance and camber, the characteristics will be shifted in vertical and/or horizontal directions. These shifts are represented by S_v and S_h respectively. Now that C and D are determining the shape and peak value, only B is left to control the stiffness. An overview of the coefficients:

- B = stiffness factor
- C = shape factor
- D = peak factor
- E = curvature factor
- S_h = horizontal shift
- S_v = vertical shift

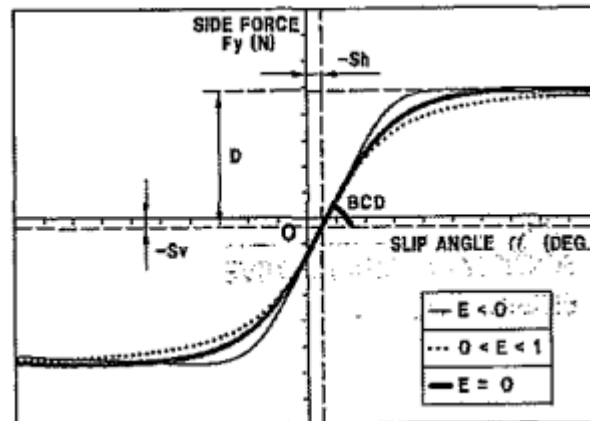


Figure 3.12: Coefficients appearing in tyre formula ¹².

The influence of the the vertical load F_z and the camber angle γ is included by writing the coefficients as a function of these quantities. The factors are all written as separate formulas which change for each characteristic. This can be found in [2].

¹¹Image taken from [19].

¹²Image taken from [19].

3.3.2. Model type

The Magic Formula is indicated in Figure 3.1. It is clear to see that this is an empirical model. The formula does not have a physical basis. It is purely based on the graph shape of measurement data. This is both its strong and weak point. It is strong because you can model every tyre with this formula. If all the parameters from a specific tyre are known, the force generation from the tyre in any situation is known. This makes it very useful for vehicle dynamic simulations. However, this makes it also its weak point. To be able to model every tyre, every tyre should be extensively measured in order to find all the parameters.

3.4. 1999 - Ftire

The development of FTire started in 1998 by Gipser [24], but certain ideas and concepts of this model go back to two other tyre models of this author: DNS-Tyre (Dynamical Non-Linear Spatial Tire Model, [25–29]), and BRIT (Brush and Ring Tire model, [29, 30]). DNS-Tire, under development since 1986, is a coarse non-linear time-domain finite element model. In the early days DNS-Tire required too much computation time to be used as a standard tyre model in full vehicle simulation. DNS-Tire contains two sub-models. The first one is the structural model of the belt, sidewall, carcass and bead. This model consists of lumped masses, connected to each other by a non-linear and an isotropic network of translational springs, dampers and bending stiffness. The model allows to select an arbitrary number of nodes both in circumferential and in lateral direction. The other sub-model is the tread model, which approximates the distributed mass, damping, stiffness and friction properties of the tread rubber.

The BRIT model was developed since 1990 as a counterpart to the DNS-Tire model. BRIT had lower computation time but had to remain accuracy, even for higher-frequent excitation. BRIT replaced DNS-Tire's time consuming stiff non-linear finite element model of the tyre structure by a simple rigid body approach, giving the belt structure six degrees of freedom of motion relative to the rim. The shape of the contact patch and the pressure distribution are approximated mathematically, as a function of camber, deflection and road surface geometry.

Due to the demand of car and tyre manufacturers for even better, faster and less restricted tyre simulations, the development of FTire started [31].

3.4.1. Force generation

As is clear by now, FTire is a finite element model. It is available in all important MBS, multi-physics system and FEA simulation environments [3]. So the forces are calculated by a finite element analysis. Just as the DNS-Tire model, this model also consists of two sub-models. One mechanical model for the belt-carcass-bead structure and another one for the mechanical and tribological properties of the tread.

The mechanical model of the belt-carcass-bead structure is implemented as a spring/damper/mass assembly. Within this assembly, the tyre belt is an extensible and flexible ring which is elastically founded on the rim by distributed, partially dynamic stiffnesses in radial, tangential and lateral direction. This is depicted in Figure 3.13.

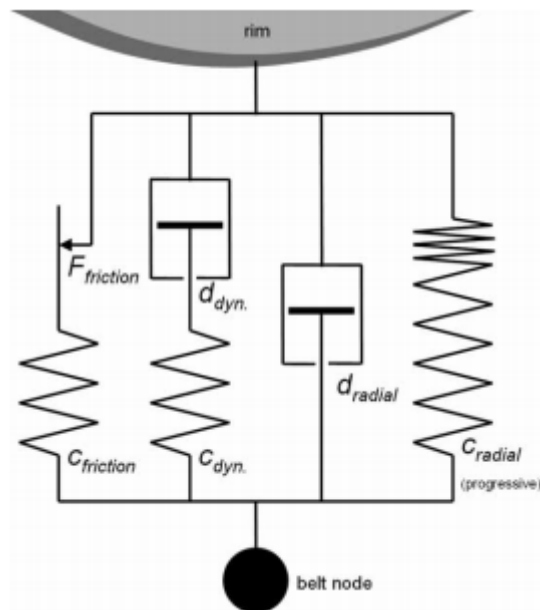


Figure 3.13: Force elements between single belt node and rim (only those in radial direction shown)¹³.

This ring has degrees of freedom such that rim in-plane as well as out-of-plane motions are possible. The ring is numerically approximated by a finite number of rigid belt elements which are coupled by stiff translational springs and by bending stiffnesses to their neighbours. This is about both the in-plane and out-of-plane directions as shown in Figure 3.14.

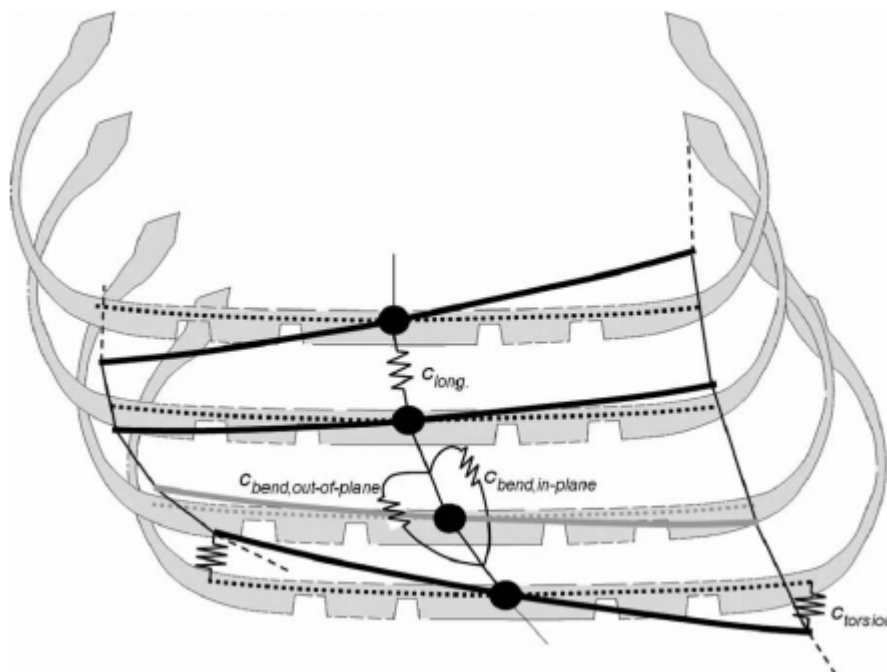


Figure 3.14: Some force elements between adjacent belt elements and rim¹⁴.

Each belt element has three translational degrees of freedom, one rotational degree of freedom and a certain number of 'bending degrees of freedom'. The bending degrees of freedom describe the

¹³Image taken from [31].

¹⁴Image taken from [31].

shape of the belt distortion caused by bending about the circumferential axis. These degree of freedom as shown in Figure 3.15.

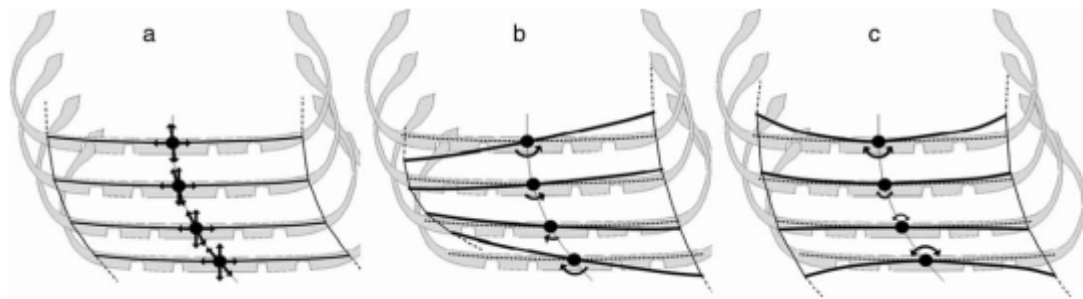


Figure 3.15: Degrees of freedom of the belt elements¹⁵.

The torsion angles are coupled by rotational stiffnesses between two adjacent belt elements and by another rotational stiffness for each belt element, located between belt element and rim. Simultaneously, a certain 'kinematic' coupling between the lateral displacement of a belt element and its torsion angle is taken into account by an appropriate coupling stiffness.

The tread sub-model is connected to every belt element. A certain number (10-100, say) of mass-less 'tread blocks' are attached to each belt element. These blocks have non-linear stiffness and damping properties in lateral, radial and tangential directions. The tangential and lateral deflections are determined by the sliding velocity on the ground and the local values of the sliding coefficient. The radial deflections of the blocks depend on road profile, locus and orientation of the associated belt elements.

Inputs of the model are position of the rim centre in the global frame, translational velocity vector of the rim centre, angular orientation of the rim in the global frame and angular rotation velocity vector of the rim. Outputs are all the forces and moments applied to the rim.

The model that has been developed over time now includes a lot more than originally. It also includes a distributed thermal model and a distributed tread-wear model. More extensions of this model can be found in [31].

3.4.2. Model type

Like mentioned before the FTire model is a finite element model. This means that it is classified as the most right model tyre in Figure 3.1. This model is applicable to any kind of tyre.

3.5. 2005 - Enhanced string model

In 2005 Meijaard and Popov present a paper in which they suggest a brush model on a two-parameter Pasternak foundation [32]. The two-parameter Pasternak foundation represents the stiffness generated by the inflation pressure, the sidewalls and the pre-stress of the tyre belt [33] and is the string in this model, which has already been used in 1922 by Wieghardt [34]. The enhanced part of this model are the bristles of the brush that represent the elements of the tread.

3.5.1. Force generation

Displacing the string in lateral and vertical directions provides a restoring force. The restoring force is given by a combination of a part that is proportional to the deflection, as in a Winkler elastic foundation, and a part that is proportional to the second derivative, the change in curvature, which is caused by the shearing of the foundation (Pasternak).

The model contains 11 parameters and some additional parameters that describe the shape of the tyre. The solution process starts with the determination of the normal force distribution. It is assumed that the distribution of the normal pressure is a function of the deflection of the tyre only and it is not influenced by the longitudinal and lateral forces in the contact patch. The length of the contact patch is an initially undetermined parameter that has to satisfy a nonlinear equation without an explicit

¹⁵Image taken from [31].

solution. This equation expresses the condition that the contact pressure vanishes at the ends of the contact line. The solution is obtained after a few numerical iterations. It is too extensive to show the equations here, for the equations read [32].

Once the normal pressure distribution is known, the steady-state longitudinal and lateral force distributions can be calculated. The inputs that are used for this are the longitudinal slip, lateral slip and the normal spin. Furthermore, the rolling velocity of the wheel, which is the velocity at which the tyre passes through the contact line, is needed. The transition points between the adhesion and sliding regions in the contact patch have to be determined by numerically solving a nonlinear equation. The resultants are the longitudinal force, lateral force and the self-aligning torque. Also these equations are too extensive to show here, so for reference check [32].

3.5.2. Model type

The enhanced string model classifies as a simple physical model in Figure 3.1. According to Meijaard the string model is particularly useful for motorcycle tyres and even more so for bicycle tyres. The contact patch has an elongated shape; that is, the contact patch is narrow, often not more than one third of the tyre width, and long, especially for narrow tyres on wheels with a larger diameter. This translates into a model where the contact patch is approximated by a line, which is a string model. The two-dimensional contact problem is reduced to a one-dimensional problem by lumping all contact elements on a meridian together in a single contact element.

3.6. 2001 - RMOD-K

In 2001 Oertel and Fandre published an article in which they introduced their tyre model RMOD-K [35]. RMOD-K is an open source collection of two simple tyre models and related subjects like optimisation tools and simulation interfaces. The goal was to build a package reaching from parameter optimisation based on measurements of steady-state force and moment to simulation models of steady-state tyre behaviour in vehicle dynamics. This can be used in situations where steady-state tyre behaviour is of interest, for instance education. The idea was to provide an algebraic formula with physical meaningful parameters and a discrete version of tangential contact formulation to get insights in tangential contact mechanics. This formula allows for instance to investigate the stability of small vehicle models by analytical linearisation even in combined slip situation. This may lead to stability maps as a function of tyre parameters. The discrete version takes into account more detailed information about normal stress distribution, contact area shape and friction properties and is able to deal with camber.

3.6.1. Force generation

The force is generated by algebraic formulas. These formulas are described in [36]. To give a fast explanation of the equations: The contact patch is a rectangle with longitudinal and lateral slip without turn slip and the normal pressure distribution is a quadratic relation in the longitudinal direction of the contact patch. The equations seem to be similar to the brush model. Further on in [36] they create an extension of the model by separating the contact patch into smaller, individual rectangular shaped contact patch segments.

3.6.2. Model type

This model is classified as a physical model in between option 3 & 4 in Figure 3.1. This model will be applicable to any kind of tyre. They start of with a simple physical model and extend it to a finite element model. However, it doesn't seem to be at the level of FTire.

3.7. 2016 - Nonlinear brush formulation for a bicycle tire based on the Rotta model

Papdopoulos and Dressel worked together on a model in which they combine two models in order to obtain a better model [4]. In their effort they weave together two classical models:

- The 'line-spring' (brush, spoke, bristle) tyre models
- Rotta's cross section model

They hope that slender bicycle tyres can be understood and modelled by a brush approach, but such a model must be nonlinear to successfully reproduce observed finite-compression camber and transverse behaviour. Rotta's analysis of section behaviour is very nonlinear and produces the needed properties directly from the tyre and wheel geometry. They devise polynomial approximations to Rotta's compression and camber analysis, then use the resulting nonlinear line spring to integrate through the contact patch, to derive expressions for the overall tyre behaviour. They also use slightly different parameters to describe Rotta's model.

3.7.1. Force generation

The force generation is exactly the same as was described by Rotta in his paper [16]. The big difference can be found where they connect the individual cross sections. Rotta used a single cross section to stand in for the entire contact patch. In this paper by Papadopoulos and Dressel they consider the entire contact patch to be made up of many slices, each with a different compression. A contact patch calculation could be performed fully numerically or semi-analytically. They discuss both in this paper.

The results of both the numerical and semi-analytical calculation are "encouragingly similar" to measurement results. However, accurate agreement was not achieved. They say that known sources of error are the pressure measurement, the tyre casing thickness (the midplane of the membrane is inwards of the rim flanges) and the changing apparent rim width due to casing wrap. Additionally, a known pressure-independent elastic contribution has not been included. The model is sufficiently sensitive to such errors that better parameter choices could potentially resolve the discrepancies.

3.7.2. Model type

The Rotta model is a geometric model which would classify as a simple physical model in the graph from Figure 3.1. The same is valid for the line-spring model. Together it is still a physical model but more complex. So it would classify a bit higher than the third position from the left in Figure 3.1. This model is only valid for tyres that have a circular cross-section, e.g. bicycles, aeroplanes and to some extent motorcycle tyres.

3.8. 2017 - Non-smooth delayed contact model

The non-smooth delayed contact model is based on the stretched-string model. Beregi studied the vibrations of a towed wheel excited by the lateral deformation of the tyre [37]. The time delay in the tyre-ground contact as well as the partial side slip are considered making it possible to capture the dynamic deformation of the contact patch centre-line with relatively low parameters and computation time. This tyre model can identify the hysteresis effect in the stability of the rectilinear motion by numerical simulations, which is not possible with the simpler quasi steady-state tyre models.

Theory of the non-smooth delayed contact model

The most commonly used tyre models are assuming quasi steady-state deformation in the contact patch. This makes it possible to introduce tyre force and aligning moment characteristics, which works well for larger speeds [2] [38]. However, for low or medium velocities these models tend to be less accurate, because the memory-effect associated to the time-delay becomes more relevant in the contact patch [39] [40]. A solution to capture this behaviour is to use additional degrees of freedom besides addressed to certain dynamic features of the tyre together with the tyre force characteristics [41]. This solution is implemented in several models, but due to the higher number of parameters these might be found less convenient for a qualitative analysis of tyre dynamics. Another solution is to use continuum-based tyre models which are capable to describe the travelling waves in the rolling tyre-ground contact. The problem is that these models lead to partial differential equations, which can be computationally costly to solve.

Beregi selected the stretched-string tyre model for his study, which can be a good compromise in this respect since for pure rolling the deformation is described by a single partial differential equation whereas it takes into account the tyre deformation outside the contact patch too, which, like mentioned before, has a relevant effect in the low velocity range. A travelling wave solution can be composed analytically for the nonlinear partial differential equation by introducing time delay distributed along the contact length. However, the travelling wave solution cannot capture the sliding effect caused by friction in the contact region. Thus, while it can be effectively used for linear stability analysis, to

investigate the nonlinear dynamics it has to be enhanced by taking the side slip into account too.

Taking the memory effect and the contact friction into account simultaneously in the tyre-road contact can result in a complex structure of sticking and sliding regions, as for the stretched-string model in particular, the deformation in the sliding parts is described by differential equations [42]. Beregi mentions that in contact mechanics several studies revealed a similar structure of sticking and sliding regions in the frictional contact of elastic continua [43]. In his study Beregi introduces a case-selective algorithm to determine the boundaries and the deformation in the different regions that can occur while the tyre makes lateral vibrations. Then the non-smooth delayed tyre model is implemented in the numerical simulation of a towed wheel. By obtaining the stable periodic solutions in the system he demonstrates the hysteresis effect observed in practice regarding the stability of the rectilinear motion.

Equations of a shimmying wheel

In their study they implement their tyre model into the in-plane model of a towed wheel attached to a rigid caster of length l , which is towed by a constant velocity V along the x -direction. The system has mass m and mass moment of inertia J_A with respect to the joint A. The deflection angle $\psi(t)$ can be used as a generalised coordinate to describe the position of the system in the (X,Y) coordinate-plane. To the king pin J a torsional damper with a damping coefficient of d_t is attached. All this is shown in Figure 3.16.

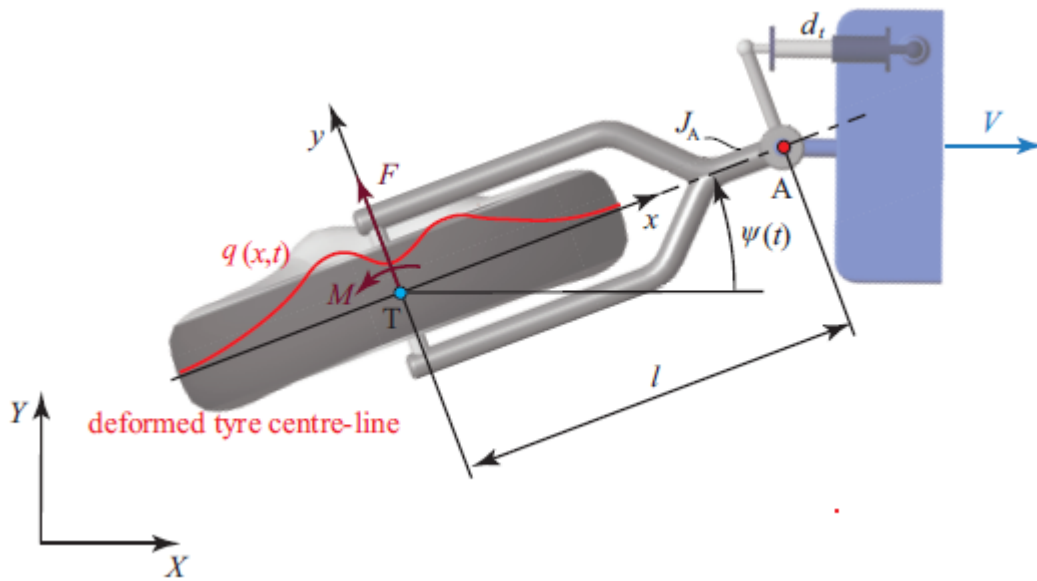


Figure 3.16: The in-plane model of a towed wheel with a rigid caster ¹⁶.

The equation of motion of the yaw vibrations of the wheel are as follows:

$$J_A \ddot{\psi}(t) + d_t \dot{\psi}(t) = M - Fl \quad (3.16)$$

where F and M are lateral contact force and aligning torque respectively. They are generated by the tyre deformation. The dots refer to time-derivatives.

¹⁶Image is taken from [37].

3.8.1. Force generation

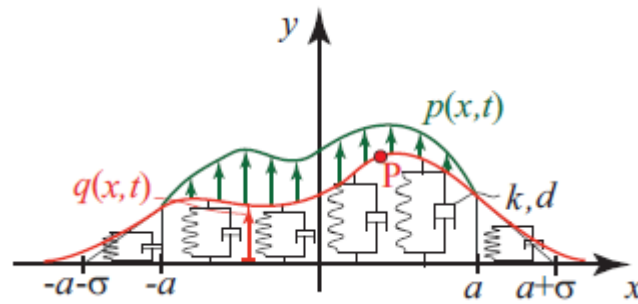


Figure 3.17: The stretched-string tyre model ¹⁷.

The tyre forces are calculated with the stretched-string tyre model, this is similar to the model from previous chapter. The difference is that instead of having only linearly distributed spring elements, this model also has linearly distributed damper elements. It is assumed that tyre damping is large enough not to allow deformation waves travelling around the wheel to have significant interference with the deformation at the leading edge $x = a$. The tyre model is shown in Figure 3.17. In the contact patch a distributed force system of $p(x, t)$ is applied to the string resulting in the deformation of the tyre, whereas outside the contact patch the tyre is assumed to be unloaded in lateral direction. The lateral deformation of the string can be described by the following partial differential equation:

$$k\sigma^2 q''(x, t) - d\dot{q}(x, t) - kq(x, t) = p(x, t) \quad (3.17)$$

where $q(x, t)$ is the lateral deformation of the string and σ is the tyre relaxation length. Primes refer to derivatives with respect to coordinate x . The tyre forces are calculated according to the classical stretched-string model by integral formulae

$$F = k \int_{-\infty}^{\infty} q(x, t) dx + d \int_{-\infty}^{\infty} \frac{d}{dt} q(x, t) dx \quad (3.18)$$

and

$$M = k \int_{-\infty}^{\infty} xq(x, t) dx + d \int_{-\infty}^{\infty} x \frac{d}{dt} q(x, t) dx. \quad (3.19)$$

3.8.2. Model type

The stretched-string model used by Beregi classifies as a simple physical model in Figure 3.1. The model is fairly similar to the model used by Meijaard and Popov. A difference compared to the enhanced string model is that the damping is also taken into account. The vertical pressure distribution is simpler again, just as with the tyre brush model. The most important difference of this model is that it also takes into account the relaxation length of the tyre. This is deformation of the string outside of the contact patch, which also generates a force. The relaxation length is an important parameter for wheel-shimmy effect at medium to low speeds[44]. There are several methods or rule of thumb to calculate/estimate the relaxation length [12] [45]. This might be useful for future calculations.

¹⁷Image is taken from [37].

4

Additional literature

In this Chapter additional literature will be discussed. The additional literature is sorted by subject. Per subject the referenced literature will be ordered chronologically.

4.1. Motorcycle research

Motorcycle tyres have similarities with bicycle tyres. They both allow for large camber angles and have a toroidal shape. However, there are also differences, such as vertical load, inflation pressure, carcass stiffness and cross section profile. The circular cross section is more valid for bicycle tyres where motorcycle tyres have a v-shaped cross section [46] or the cross section is defined by multiple radii [31]. The information found on motorcycle tyres might be useful further on in this research, so the noteworthy references will be mentioned in this section.

4.1.1. 1971 - R.S. Sharp

In 1971 Sharp publishes a paper about the stability and control of motorcycles [47]. This paper is mainly about the mathematical models of a motorcycle dependent on three alternative assumptions concerning the tyre behaviour. The stability characteristics deduced from these three assumptions are compared.

Sharp uses a normalised cornering stiffness of 0.191 to 0.195 per degree of slip angle. The normalised camber stiffness that he uses is from 0.0161 to 0.0163 per degree of camber. The pneumatic trail is neglected.

4.1.2. 1976 - R.S. Rice and D.T. Kunkel

In a report from the Calspan Corporation Rice and Kunkel describe a brief study of motorcycle handling characteristics using both analytical and experimental methods [48]. Their objective was to supplement the results of a much broader earlier study on motorcycle accident avoidance capabilities in three areas, namely: (1) Demonstration of the motorcycle/rider dynamic simulation in a transient handling task (single lane change). (2) Acquisition of additional data on motorcycle controllability as evaluated by torque sensitivity parameters. (3) Lane change testing of additional riders to identify differences in riding technique.

In the report they mention that the measured motorcycle tyres were "smooth, universal and ribbed". The tyres were inflated "according to manufacturer's recommendation" and with a vertical load of "nominal value with a 200 lb. rider and a 120% of the nominal value", a normalised cornering stiffness of 0.33 to 0.15 per degree of slip angle was measured. A normalised camber stiffness of 0.009 to 0.21 per degree of camber angle was reported. The pneumatic trail was between 13 and 25 mm. They reported that for a given tyre, the value of the cornering stiffness coefficient decreased as the normal load increased. The value of the camber stiffness was relatively unaffected by the normal load.

4.1.3. 1979 - H. Sakai, O. Kanaya and H. Iijima

In 1979 an article on the effect of main factors on dynamic properties of motorcycle tyres was published [49]. The study was intended to clarify how various tyre conditions such as internal pressure, load, tyre

make, width, tread pattern, tread curvature and the drum curvature influence the dynamic properties of motorcycles tyres.

They report a normalised camber stiffness of 0.0176 per degree of camber. This is a slightly higher than the tangent rule.

4.1.4. 1998 - E.J.H. De Vries and H.B. Pacejka

De Vries and Pacejka published an article in 1998 in which they report on measurements they did for Pirelli, BMW and Marzocchi [50]. This research was carried out in order to improve the MF-tyre model to fit the road measurements accurately at large camber angles and to ensure a consistent behaviour outside the measured domain.

In this report it is written that a 120/70 front tyre under a vertical load of 1600 to 3200 N has a normalised cornering stiffness of 0.125 to 0.225 per degree of slip angle and a normalised camber stiffness of 0.0268 to 0.069 per degree of camber.

4.1.5. 2002 - R. Berrirra, V. Cossalter A. Doria and Lot

In the paper a paper from 2002, Berrirra et al. describe an experimental research program to quantify the concept of 'relaxation length' of the rolling, steered and cambered motorcycle tyre [51]. They tested many cross-ply and radial-ply tyres with different tread and ply materials. The experimental data obtained from the rotating disk machine is analysed using a mathematical model.

On the motorcycle tyre testing device they found a normalised cornering stiffness of 0.1 to 0.25 per degree of slip angle and a normalised camber stiffness of 0.015 to 0.02 per degree of camber angle. These were the most extreme values reported, depending on tyre, vertical load and inflation pressure the results are varying between these values.

4.2. Books

4.2.1. 1981 - Mechanics of pneumatic tires

In 1981 Clark published a book about the mechanics of pneumatic tyres [52]. In this book he bundled all the information that was found on pneumatic tyres until that point. He discusses subjects like: rubber structure and properties, rubber and cord bonding, tyre structure, contact between tyre and road, traction, stress and deformation, measurement of tyre properties and the analysis of tyre properties. In case of necessity this is a nice reference to check back at.

4.2.2. 2006 - The pneumatic tire

In 2006 a book is published which is a rewritten version of Clark's "Mechanics of pneumatic tires" [53]. For many years tyre engineers relied on the work of Clark for detailed information about the principles of tyre design and use. While many subjects in that book are still relevant, there are also parts that need revision and extensions should be added due to the advancements in tyre technology through the years.

4.3. Miscellaneous

4.3.1. 1991 - Pacejka and Sharp

In 1991 Pacejka and Sharp published an article in which they analyse the shear force development by pneumatic tyres in steady-state conditions [54]. They do this on the basis of, at that time, available models. They review the different modelling methods like the ones that are shown in Figure 3.1 (Empirical models, models using the similarity method, simple physical models and complex physical models which require computer simulation). For every modelling method they explain the different available models within that method. In the end they draw conclusions about the structural and frictional mechanisms present in the shear force generation process, the contributions of carcass and tread elastic properties and of geometrical and frictional factors to the determination of the distributions of force through the contact region, the relationship between accuracy and computational load and the selection of methods for modelling tyre forces in a road vehicle dynamics context.

5

Conclusions

A lot of research has been done on tyres. However, there is not so much complete data available for bicycle tyres. The research done by Dressel and the bachelor group adds a lot of valuable data to what is actually available. This data will be used in the main Master thesis research.

The amount of available tyre models is large. As has been explained in this literature research, there are various methods for tyre modelling. The models that classify as simple physical models in Figure 3.1, will be elaborated further in the Master thesis report. The goal is to use one of these models and find the model parameters corresponding to the measurements done by Dressel and the bachelor group. Hopefully it will be possible to make an estimation for the behaviour of other bicycle tyres on the basis of the found model parameters.

Bibliography

- [1] A. E. Dressel, *Measuring and modeling the mechanical properties of bicycle tires*, Ph.D. thesis, The University of Wisconsin-Milwaukee (2013).
- [2] H. B. Pacejka, *Tire and Vehicle Dynamics* (Elsevier Ltd., Oxford, United Kingdom, 2012).
- [3] *Ftire*, (2018), <https://www.cosin.eu/>.
- [4] J. Papadopoulos and A. E. Dressel, *Nonlinear brush formulation for a bicycle tire based on rotta model*, in *Bicycle and Motorcycle Dynamics* (2016).
- [5] J. Knuit, F. de Kok, P. Raaphorst, and A. van der Spek, *Bicycle tire stiffness and damping*, (2014), bachelor Thesis.
- [6] R. D. Roland and J. P. Lynch, *Bicycle Dynamics: Tire Characteristics and Rider Modeling* (Cornell Aeronautical Laboratory, 1972).
- [7] J. Davis, *Bicycle tire testing-effects of inflation pressure & low coefficient surfaces*, Calspan Report No. ZN-5431-V-3, 1975 (1975).
- [8] G. K. Man and T. R. Kane, *Steady turning of two-wheeled vehicles*, SAE Transactions , 715 (1979).
- [9] C. R. Kyle, *GM tire test report on 17" moulton tires*, Technical report (General Motors, 1987).
- [10] C. Kyle, *Sunraycer, wheels, tires and brakes*, Sun-raycer Design Notebook, General Motors Corporation, Detroit (1988).
- [11] D. Cole and Y. Khoo, *Prediction of vehicle stability using a "back to back" tyre test method*, International Journal of Vehicle Design **26**, 573 (2001).
- [12] V. Cossalter, *Motorcycle Dynamics* (Lulu.com, Morrisville, North Carolina, USA, 2006).
- [13] V. Cossalter, A. Doria, R. Lot, N. Ruffo, and M. Salvador, *Dynamic properties of motorcycle and scooter tires: Measurement and comparison*, Vehicle system dynamics **39**, 329 (2003).
- [14] R. S. Sharp, *On the stability and control of the bicycle*, Applied mechanics reviews **61** (2008).
- [15] A. Doria, M. Tognazzo, G. Cusimano, V. Bulsink, A. Cooke, and B. Koopman, *Identification of the mechanical properties of bicycle tyres for modelling of bicycle dynamics*, Vehicle system dynamics **51**, 405 (2013).
- [16] J. Rotta, *Zur statik des luftreifens*, Ingenieur-Archiv **17**, pp. 129 (1949).
- [17] J. Rotta, *On the statics of the pneumatic tire*, (1952), (Zur Statik des Luftreifens). Translated by R.E. Frank, Cornell Aeronautical Laboratory, Inc., February 1952.
- [18] H. B. Pacejka, *Spin: camber and turning*, Vehicle System Dynamics **vol. 43**, pp. 3/17 (2005).
- [19] E. Bakker, H. B. Pacejka, and L. Lidner, *A new tire model with an application in vehicle dynamics studies*, Tech. Rep. (SAE technical paper, 1989).
- [20] H. B. Pacejka and E. Bakker, *The magic formula tyre model*, Vehicle system dynamics **21**, 1 (1992).
- [21] L. Lidner, *Experience with the magic formula tyre model*, Vehicle System Dynamics **21**, 30 (1992).
- [22] J. J. van Oosten and E. Bakker, *Determination of magic tyre model parameters*, Vehicle System Dynamics **21**, 19 (1992).

- [23] H. Pacejka and I. Besselink, *Magic formula tyre model with transient properties*, Vehicle system dynamics **27**, 234 (1997).
- [24] M. Gipser, *Ftire, a new fast tire model for ride comfort simulations*, in *International ADAMS User's Conference, Berlin, Germany* (1999).
- [25] M. Gipser, *Dns-tire, ein dynamisches, räumliches nichtlineares reifenmodell*, Reifen, Fahrwerk, Fahrbahn. VDI Berichte **650**, 115 (1987).
- [26] M. Gipser, *Dns-tire, a dynamic nonlinear spatial tire model in vehicle dynamics*, in *Proc. 2nd Workshop on Road-Vehicle-Systems and Related Mathematics, ISI, Torino Italy* (1987).
- [27] M. Gipser, *Dns-tire 3.0-die weiterentwicklung eines bewährten strukturmechanischen reifenmodells*, FORTSCHRITT BERICHTE-VDI REIHE 12 VERKEHRSTECHNIK FAHRZEUGTECHNIK , 52 (1996).
- [28] M. Gipser, *Reifenmodelle fuer komfort-und schlechtwegsimulation*, in *7. AACHENER KOLLOQUIUM FAHRZEUG-UND MOTORENTECHNIK, 5.-7. OKTOBER 1998* (1998).
- [29] M. Gipser, *Pneumatic tire models: the detailed mechanical approach*, Road and off-road vehicle system dynamics handbook , 625 (2013).
- [30] M. Gipser, R. Hofer, and P. Lugner, *Dynamical tyre forces response to road unevennesses*, Vehicle System Dynamics **27**, 94 (1997).
- [31] M. Gipser, *Ftire—the tire simulation model for all applications related to vehicle dynamics*, Vehicle System Dynamics **45**, 139 (2007).
- [32] J. P. Meijaard and A. A. Popov, *Tyre modelling for motorcycle dynamics*, Vehicle System Dynamics **vol. 43**, pp. 187 (2005).
- [33] V. Z. Vlasov, *Beams, plates and shells on elastic foundation*, Israel Program for Scientific Translation (1966).
- [34] K. Wieghardt, *Über den balken auf nachgiebiger unterlage*, ZAMM-Journal of Applied Mathematics and Mechanics/Zeitschrift für Angewandte Mathematik und Mechanik **2**, 165 (1922).
- [35] C. Oertel and A. Fandre, *Das reifenmodellsystem rmod-k*, ATZ-Automobiltechnische Zeitschrift **103**, 1074 (2001).
- [36] C. Oertel, *RMOD-K Formula Documentation*, Tech. Rep. (Brandenburg University of Applied Sciences, Faculty of Engineering, 2011).
- [37] S. Beregi and D. Takács, *Analysis of the tyre-road interaction with a non-smooth delayed contact model*, in *Rolling Contact Mechanics for Multibody System Dynamics* (2017).
- [38] G. Rill, *Tmeasy - the handling tire model for all driving situations*, in *Proceeding of the XV International Symposium on Dynamic Problems of Mechanics* (2013).
- [39] D. Takács, G. Orosz, and G. Stépán, *Delay effect in shimmy dynamics of wheels with stretched string-like tyres*, European Journal of Mechanics A/Solids **28**, pp. 516 (2009).
- [40] D. Takács and G. Stépán, *Contact patch memory of tyres leading to lateral vibrations of four-wheeled vehicles*, Philosophical Transactions of the Royal Society A: Mathematical Physical and Engineering Sciences **vol 371** (2013).
- [41] P. Lugner, H. B. Pacejka, and M. Plöchl, *Recent advances in tyre models and testing procedures*, Vehicle System Dynamics **vol. 43**, pp. 413 (2005).
- [42] D. Takács and G. Stépán, *Micro-shimmy of towed structures in experimentally uncharted unstable parameter domain*, Vehicle System Dynamics **vol. 50**, pp. 1613 (2012).

- [43] A. Thaitirarot, R. Flicek, D. A. Hills, and J. R. Barber, *The use of static reduction in the solution of two-dimensional frictional contact problems*, Journal of Mechanical Engineering Science **vol. 228**, pp. 1474 (2014).
- [44] P. W. A. Zegelaar, *The dynamic response of tyres to brake torque variations and road unevennesses*, Ph.D. thesis, Delft University of Technology (1998).
- [45] R. T. Uil, *Non-lagging effect of motorcycle tyres: An experimental study with the Flat Plank Tyre Tester*, Tech. Rep. (Eindhoven University of Technology, 2006).
- [46] A. Waheed, *Michelin power one race tire review*, MotorcycleUSA (2011).
- [47] R. S. Sharp, *The stability and control of motorcycles*, Journal of mechanical engineering science **13**, 316 (1971).
- [48] R. S. Rice, J. A. Davis, and D. T. Kunkel, *Accident-avoidance capabilities of motorcycles*, Tech. Rep. (NTIS, 1976).
- [49] H. Sakai, O. Kanaya, and H. Iijima, *Effect of main factors on dynamic properties of motorcycle tires*, SAE Transactions , 892 (1979).
- [50] E. d. De Vries and H. Pacejka, *Motorcycle tyre measurements and models*, Vehicle System Dynamics **29**, 280 (1998).
- [51] R. Berritta, V. Cossalter, A. Doria, and N. Ruffo, *Identification of motorcycle tire properties by means of a testing machine*, in *SEM Conference Milwaukee* (2002).
- [52] S. K. Clark, *Mechanics of Pneumatic Tires* (Department of Transportation, National Highway Traffic Safety Administration, Washington DC, US, 1981).
- [53] A. N. Gent and J. D. Walter, *Pneumatic tire* (Department of Transportation, National Highway Traffic Safety Administration, Washington DC, US, 2006).
- [54] H. B. Pacejka and R. S. Sharp, *Shear force development by pneumatic tyres in steady state conditions: a review of modelling aspects*, Vehicle system dynamics **20**, 121 (1991).